MODELLING OF REACTIVE TRANSPORT IN A SEDIMENTARY BASIN AFFECTED BY A GLACIATION/DEGLACIATION EVENT

Sergio A. Bea, K. Ulrich Mayer
University of British Columbia, Dept. of Earth and Ocean Sciences
Vancouver, BC, Canada

Kerry T.B. MacQuarrie
University of New Brunswick, Dept. of Civil Engineering
Fredericton, NB, Canada

ABSTRACT

Canada's plan for the long-term care of used nuclear fuel is containment and isolation in a Deep Geologic Repository (DGR) constructed in a suitable sedimentary or crystalline rock formation. In sedimentary basins fluid migration and geochemical conditions may be impacted by multiple interacting processes including density-dependent groundwater flow, solute transport, heat transfer, mechanical loading, and rock-water interactions. Understanding the interactions among these processes is important when assessing the long-term hydrodynamic and geochemical stability of sedimentary basins during glaciation/deglaciation events. To improve the capability to investigate these processes, an enhanced version of the reactive transport code MIN3P (i.e. MIN3P-NWMO) was developed and tested. The processes incorporated in the new model were evaluated by simulating reactive transport in a hypothetical sedimentary basin affected by a simplified glaciation scenario consisting of a single cycle of ice sheet advance and retreat. The simulations are used to provide an illustrative assessment of the hydrogeological and geochemical stability of this sedimentary basin over a time period of 32,500 years. The results suggest a high degree of geochemical stability.

1. INTRODUCTION

The Canadian Nuclear Waste Management Organization (NWMO) is responsible for implementing Adaptive Phased Management (APM), Canada's plan for the long-term care of used nuclear fuel produced by Canada's nuclear reactors. The goal of APM is containment and isolation of used nuclear fuel in a Deep Geologic Repository (DGR) constructed in a suitable sedimentary or crystalline rock formation.

In North America, many sedimentary basins have been subjected to periodic glaciation-deglaciation events (e.g. [1], [2], [3], [4], [5]). It is therefore expected that a DGR located within a sedimentary rock setting in Canada will be subject to similar events in the future. The regional buildup of significant fluid pressures below glaciers, in particular under conditions of glacial retreat (e.g. [6]), provide a potential driving force for meltwater ingress into the sedimentary rock units, although flow to deeper formations may be limited by the low permeability and subhorizontal layering of the sedimentary units, porosity and permeability reduction with depth, and the high density of basal brines.

Present day geochemical signatures confirm that glacial waters have entered shallow aquifers in sedimentary basins. For example, McIntosh and Walter [3] provide evidence that meltwater recharged through confined Silurian-Devonian aquifers at the margins of both the Illinois and

Michigan basins. Using elemental and isotope geochemistry of groundwaters in Silurian-Devonian carbonate and glacial drift aquifers, McIntosh and Walter [3] suggest that groundwater geochemistry has been altered by incongruent dissolution of carbonate minerals, dissolution of halite and anhydrite, cation exchange, microbial processes and mixing with brines.

The findings of McIntosh and Walter [3] demonstrate that the ingress of glacial waters into sedimentary rock sequences is not a conservative process. Solutes interact with clays or oxides, and mineral dissolution-precipitation reactions affect the groundwater and rock composition. Mineral dissolution and precipitation may also result in modifications to physical properties (e.g. porosity and permeability), that in turn, may influence fluid flow. Despite the fact that rock-water interactions affect the geochemical evolution in sedimentary basins, very little work has been performed to quantitatively assess these interactions using numerical simulations.

2. OBJECTIVES AND APPROACH

A key objective of the APM Geoscience research program is to further understanding of geosphere evolution and stability, including potential geosphere responses to glaciations. This work focuses on the development of a numerical model that is capable of simulating flow and reactive transport in sedimentary basins affected by glaciation/deglaciation events over time periods ranging from 10,000-100,000 years. To this end, a new numerical model (entitled MIN3P-NWMO) was developed based on the multicomponent reactive transport code MIN3P [7] and a more recent version that had been modified to include density coupling between groundwater flow and solute transport (MIN3P-D, [8]).

The capabilities of the resulting model were evaluated based on simulations conducted for a two-dimensional cross section of a generic sedimentary basin. The simulations considered coupling between density-driven flow and reactive solute transport, rock-water interaction including mineral dissolution-precipitation and ion exchange, hydromechanical coupling due to ice-sheet loading, porosity and permeability variability with depth, as well as transient boundary conditions resulting from the advance and retreat of an ice sheet. As a secondary objective, the simulation results were used to provide an illustrative assessment of the hydrogeological and geochemical stability of sedimentary basins during a glaciation event.

3. MODEL FORMULATION AND VERIFICATION

The MIN3P-D code [8] simulates groundwater flow, solute transport, and geochemical reactions under variable density conditions for solutions with maximum ionic strengths similar to sea water. However, this code is not suitable for simulating processes in more concentrated solutions and brines, which are present in many sedimentary basins. Thermal effects, for example resulting from a geothermal gradient or ingress of cold meltwater, are also not considered. In addition, the feedback between glacial loading and groundwater flow, induced during ice sheet advance and retreat, is not included in MIN3P-D.

In order to more adequately simulate the processes occurring in sedimentary basins it was necessary to implement additional processes into MIN3P-D, resulting in MIN3P-NWMO. The revised code includes the Harvie-Moller-Weare model (HMW, [9]) for the calculation of activity corrections (based on [10]) in solutions with ionic strengths up to about 20 mol l^{-1}. Fluid density calculations are based on fluid volumetric predictions derived from the Pitzer equations according to [11], which is particularly suitable for coupling density-driven flow and reactive transport involving dense brines. To account for fluid pressure changes induced by ice sheet loading, the one-dimensional hydromechanical coupling formulation presented by Neuzil [12] is included. Lastly, a numerical formulation for heat (energy) transport is coupled with the fluid and reactive transport equations following the approach of Voss and Provost [13]. After code modifications were implemented, MIN3P-NWMO was verified by revisiting benchmark problems developed using MIN3P and MIN3P-D. In addition, the new capabilities of MIN3P-NWMO were verified and tested in relation to other similar models cited in the literature and available analytical solutions. A detailed documentation of the model formulation and verification can be found in Bea et al. [14].

4. MODEL SETUP FOR SEDIMENTARY BASIN SIMULATION

4.1 Conceptual Model

The evaluation of the model capabilities is based on the simulation of flow and reactive transport in a two-dimensional cross section of a hypothetical sedimentary basin (Figure 1) that includes the key regionally-extensive features of several sedimentary basins located in eastern North America. These sedimentary basins (e.g. the Illinois, Michigan, and Appalachian basins) typically contain Paleozoic sequences of limestones and dolostones interbedded with shales and sandstones [3], where the carbonate and sandstone units constitute the main aquifers. Thick sequences of bedded evaporite units, mainly composed of halite and anhydrite, are also common (e.g. Michigan and Appalachian basins, [3]).

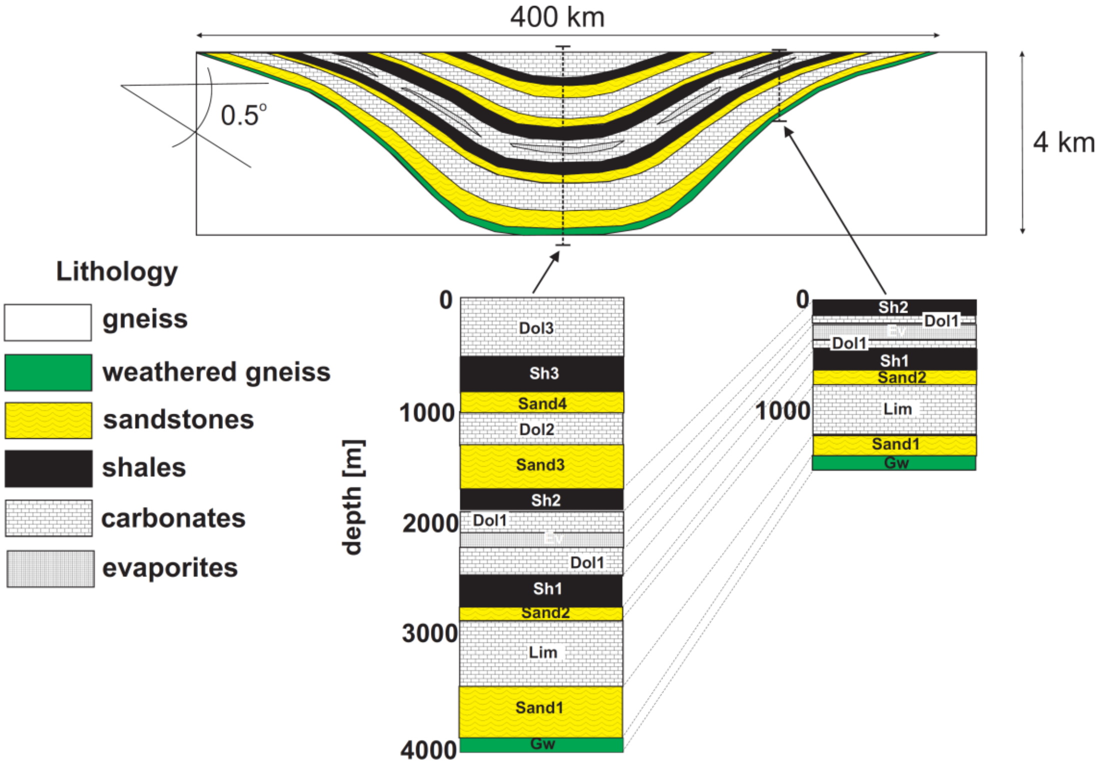

Figure 1. Geometry and main hydrogeologic units considered in the hypothetical sedimentary basin simulation

The symmetrical sedimentary basin is about 400 km in length and has a maximum depth of 4 km. It contains a sequence of carbonates (dolostones and limestones, Dol1, Dol2, Dol3 and Lim1, Figure 1) interbedded with sandstones (Sand1, Sand2, Sand3 and Sand4, constituting the main aquifers) and shales (Sh1, Sh2, Sh3, constituting the main confining units). The sedimentary formations overlay the Precambrian basement gneiss (G); it is assumed that a weathered zone of the basement crystalline rock (weathered gneiss, Gw, Figure 1) is in direct contact with the lowest sedimentary unit. To provide a comprehensive scenario, noncontiguous evaporite units (Ev) are present in one of the dolostone units (Dol1). Unconsolidated glacial drift is not considered in the current conceptual model.

In order to illustrate the potential hydrogeological and geochemical perturbations generated by ice sheet movement over the sedimentary basin described above, a simplified glaciation scenario is applied. The scenario consists of a single cycle of cold-based ice sheet advance, followed by a stable glacial maximum, with subsequent warm-based ice sheet retreat. The scenario is subdivided into four stages following the approach presented by Bense and Person [6]. The scenario is depicted in Figure 2 and consists of: Stage I, linear ice sheet accumulation, i.e. ice sheet advance (12500 years); Stage II, constant ice sheet thickness (5000 years); Stage III, melting, i.e. ice sheet retreat (5000 years); and Stage IV, no ice sheet present. The maximum ice sheet thickness and extent used in the current study are 2 km and 440 km, respectively, which implies complete ice coverage of the basin during the Stage II glacial maximum.

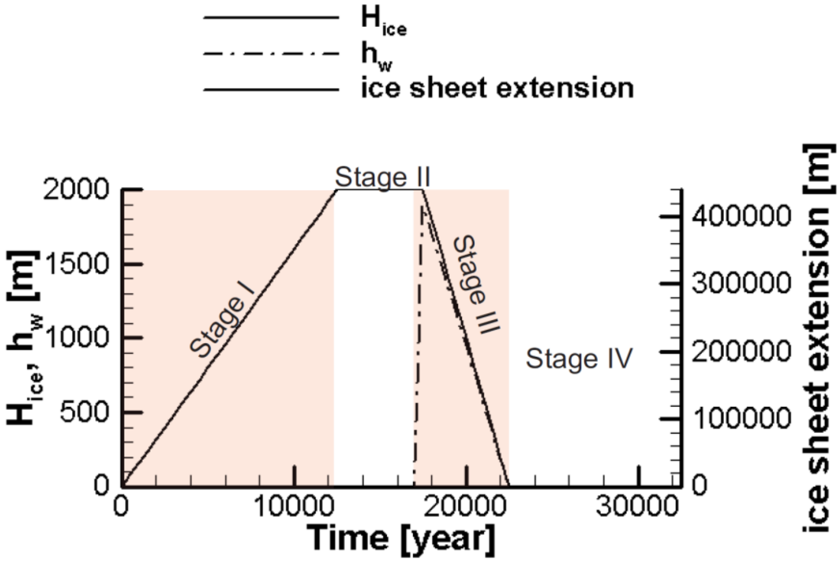

Figure 2. Glaciation scenario used to specify boundary conditions at the surface of the sedimentary basin domain, where: H_{ice} is the maximum ice sheet thickness at the right-hand edge of the domain (Figure 1); the ice sheet extension is measured from the right-hand edge of the domain; and h_w is the hydraulic head imposed at the right-hand edge of the domain during warm-based conditions (Stage III)

During Stages I, III and IV, prescribed hydraulic head boundary conditions representing topographically-driven flow are imposed on the upper boundary of the model domain where ice is not present, with the hydraulic head varying linearly from zero to a maximum of 100 m at the center of the basin. The recharge boundary conditions for solute transport on the upper ice-free domain boundary are computed based on the water flux and chemical composition of meteoric water. During the stages of accumulation and constant ice sheet thickness (Stages I and II, Figure 2), a cold-based condition is assumed and no flux of water or solutes is permitted beneath the ice sheet. During Stage III, a prescribed hydraulic head equal to 0.95 of the ice thickness is applied beneath the ice sheet (Figure 2). Solute fluxes beneath the ice sheet during Stage III are computed based on the water flux and specified meltwater chemical composition.

For the simulation considered here, it is assumed that geochemical reactions in the domain are limited to aqueous complexation, cation exchange, and dissolution/precipitation reactions involving halite, anhydrite, dolomite, and calcite. Isothermal conditions are also assumed; the influence of non-isothermal conditions on the system evolution has been considered as part of a sensitivity analysis as described in [14].

4.2 Model Parameterization

Hydrogeological properties for the rock units in Figure 1 were derived from a literature review and incorporate data reported for several sedimentary basins in North America ([5], [15], [16], [17], [18], [19], [20], [21], [22]). Representative values for several key hydrogeological properties (i.e. porosity, ø; horizontal hydraulic conductivity, K_H; vertical hydraulic conductivity, K_V; and specific storage, S_S) are provided in Table 1.

Table 1: Selected hydrogeological parameters. Values are given for a location corresponding to the center of the sedimentary basin.

Unit	Lithology	Depth [m]	ø [-]	$\log_{10} K_H$ [m s^{-1}]	$\log_{10} K_v$ [m s^{-1}]	S_S [m^{-1}]
Dol3	Dolostone	200	0.027	-6.3	-7.3	3.1×10^{-7}
Sh3	Shale	700	0.102	-11.0	-12.0	1.1×10^{-6}
Sand4	Sandstone	900	0.124	-5.7	-5.7	9.2×10^{-7}
Dol2	Dolostone	1100	0.016	-7.0	-8.0	2.6×10^{-7}
Sand3	Sandstone	1500	0.100	-6.0	-6.0	8.1×10^{-7}
Sh2	Shale	1800	0.057	-11.8	-12.8	8.9×10^{-7}
Dol1	Dolostone	2000	0.009	-12.7	-13.7	2.3×10^{-7}
Ev	Evaporites	2150	0.019	-14.9	-15.9	4.5×10^{-7}
Sh1	Shale	2500	0.039	-14.4	-15.4	8.1×10^{-7}
Sand2	Sandstone	2800	0.063	-6.4	-7.4	6.5×10^{-7}
Lim	Limestone	3200	0.005	-13.7	-14.7	1.9×10^{-7}
Sand1	Sandstone	3700	0.045	-6.8	-7.8	5.7×10^{-7}
Gw	Weathered Gneiss	3950	0.002	-12.9	-13.9	5.4×10^{-7}

Many physical parameters in sedimentary basins are expected to decrease with depth as overlying sediments compress the underlying material. Following the approach of Person et al. [23], an exponential relationship is used to represent the decline of porosity, ø, with depth. The depth dependence of the hydraulic conductivities is related to porosity using the Carman-Kozeny relationship. As discussed in [14], the depth dependence of other parameters such as the specific storage and hydromechanical loading parameters are determined in a similar fashion. This approach captures the general trends which are known to exist in compacted sedimentary rocks (e.g. [24]) and is well suited for the illustrative large-scale simulations conducted for this study.

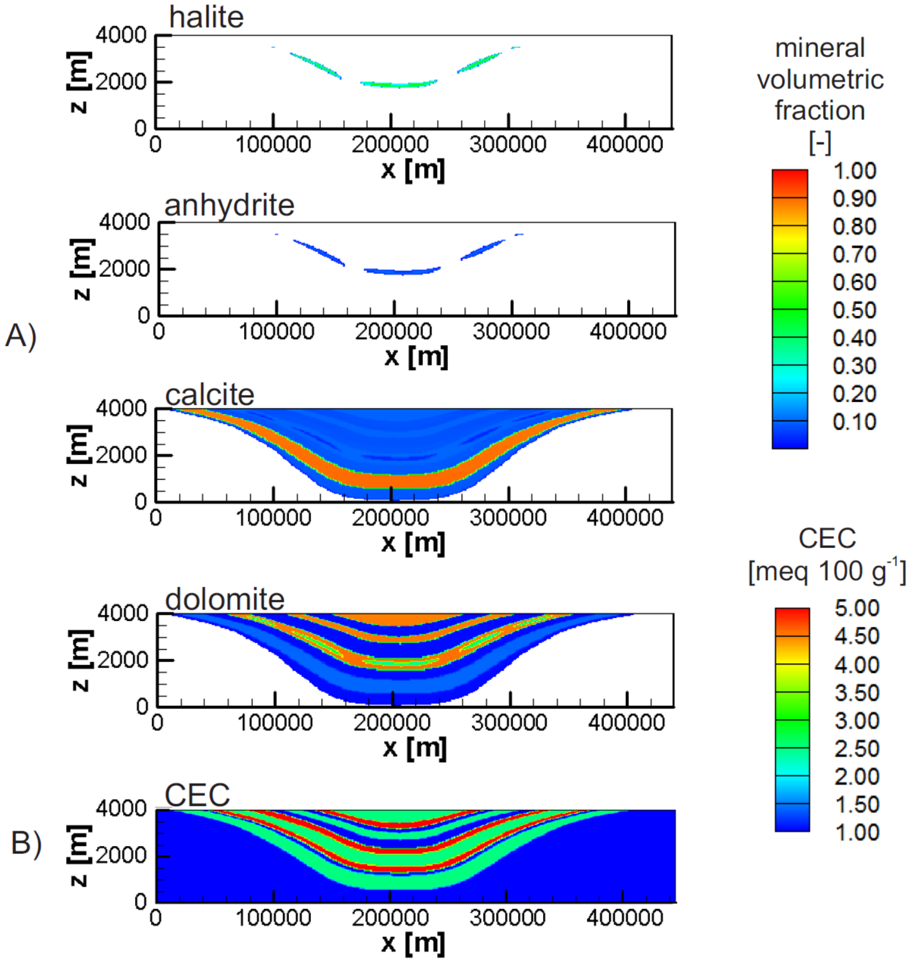

Figure 3. Initial distributions of: A) reactive minerals, and B) cation exchange capacity (CEC)

Other parameters required to populate the model include rock bulk density, solution composition and density, cation exchange capacity (CEC) and the mineralogical composition of the rock formations. The initial volume fractions for the reactive mineral phases and the CEC distribution of each geological unit are depicted in Figure 3. Calcite and dolomite are most abundant in the limestone and dolostone units, but are present in all sedimentary units. The presence of anhydrite and halite is assumed to be restricted to the evaporite units. Shale aquitards are characterized by relatively high CEC values, compared to limestone-dolostone aquifers and evaporite aquitards. Each unit is populated with a unique pore water composition [14]; fresh to brackish waters are predominant in shallow formations (less than ~ 100 m), while concentrated brines with densities exceeding 1.2 kg L^{-1} are present at greater depth. The model domain was discretized using 45,000 cells; 450 cells equidistantly distributed in the lateral direction, and 100 cells distributed in the vertical direction. The upper part of the model was refined in order to capture the dynamics of the processes in the shallow units.

5. RESULTS AND DISCUSSION

5.1 Groundwater flow and fluid density

During Stage I (i.e. ice sheet advance), point pressure heads throughout the majority of the basin increase due to the hydromechanical effects of ice sheet loading (Figure 4B). The magnitudes of the pressure head changes depend primarily on the hydraulic conductivity and hydromechanical loading coefficient assigned to the various hydrogeological units. For example at the centre of the basin at a time of 10000 yr (Figure 4B), larger pressure head differentials are induced in the intervals between 2200 and 1400 m, and between 700 and 1100 m from the basin basement; these intervals contain the units Dol1, Ev, Sh1, and Lim, respectively (Figure 1). The reason for the relatively large pressure head increases in these units is that they possess some of the lowest hydraulic conductivites (approximately 10^{-13} to 10^{-15} m s^{-1}; Table 1) and highest loading coefficients (approximately 0.8 to 0.9) in the hypothetical sedimentary rock sequence. At 10000 yr the horizontal components of Darcy velocity in Sand1 and Sand2, at a location corresponding to the center of the basin, are 1.3×10^{-2} m yr^{-1} and 3.0×10^{-2} m yr^{-1}, respectively.

The results for Stage I suggest that the pressure increases in low hydraulic conductivity units (i.e. aquitards) could induce some groundwater flow from the aquitards into adjacent aquifers of higher hydraulic conductivity. Person et al. [25] have also predicted, for a cold-based ice sheet overriding a sedimentary basin containing a sequence aquifers and aquitards, that vertical leakage would occur out of confining units into adjacent aquifers. For the results obtained here, an initial assessment of the impact of such leakage on water composition during the first 10000 yr of Stage I can be made by examining the simulated fluid density changes, which are a reflection of total dissolved solids (TDS) and thus general water composition. It is seen that the density distribution at 10000 yr is essentially identical to the initial conditions (e.g. Figure 5A and B). However, it must be noted that because this is a reactive transport simulation, fluid density can also be affected by geochemical processes.

Near the beginning of Stage III (i.e. 18000 yr), pressure heads increase in shallow permeable units (Figure 4C) as a consequence of the re-established hydraulic connection between the now warm-based melting ice sheet and these sedimentary units. Some of the highest Darcy velocities (e.g. on the order of 0.1 to 1.0 m yr^{-1}) are generated in the shallow aquifers during the early stages of glacial retreat. At 18000 yr the horizontal Darcy velocities in the deepest section (i.e. center of basin) of the Sand1 and Sand2 aquifers are also increased to 4.3×10^{-2} m yr^{-1} and 2.3×10^{-1} m yr^{-1}, respectively. The most substantial recharge and discharge fluxes for the basin are also predicted during this stage, despite the fact that only a small fraction of the meltwater (~ 0.4%, calculated for Stage III (17,500 - 22,500 years) and based on an ice density of 850 kg m^{-3}) is able to enter the basin as recharge. These pressure head and specific discharge changes are not, however, significant enough to perturb the fluid density in the vast majority of the basin (e.g. Figure 5C). The only regions of notable meltwater ingress are in the shallow aquifers Dol2 (x=133000 m; Figure 5C) and Sand4 (x=278000 m; Figure 5C) where isolated plumes of fresh water reach depths of approximately 350 m and 320 m, respectively.

During Stage IV (i.e. inter-glacial period), point pressure heads in the basin have essentially returned to the initial conditions (Figure 4E). The fluid density distribution below a depth of approximately 300 m is also essentially the same as the initial distribution (Figure 5E).

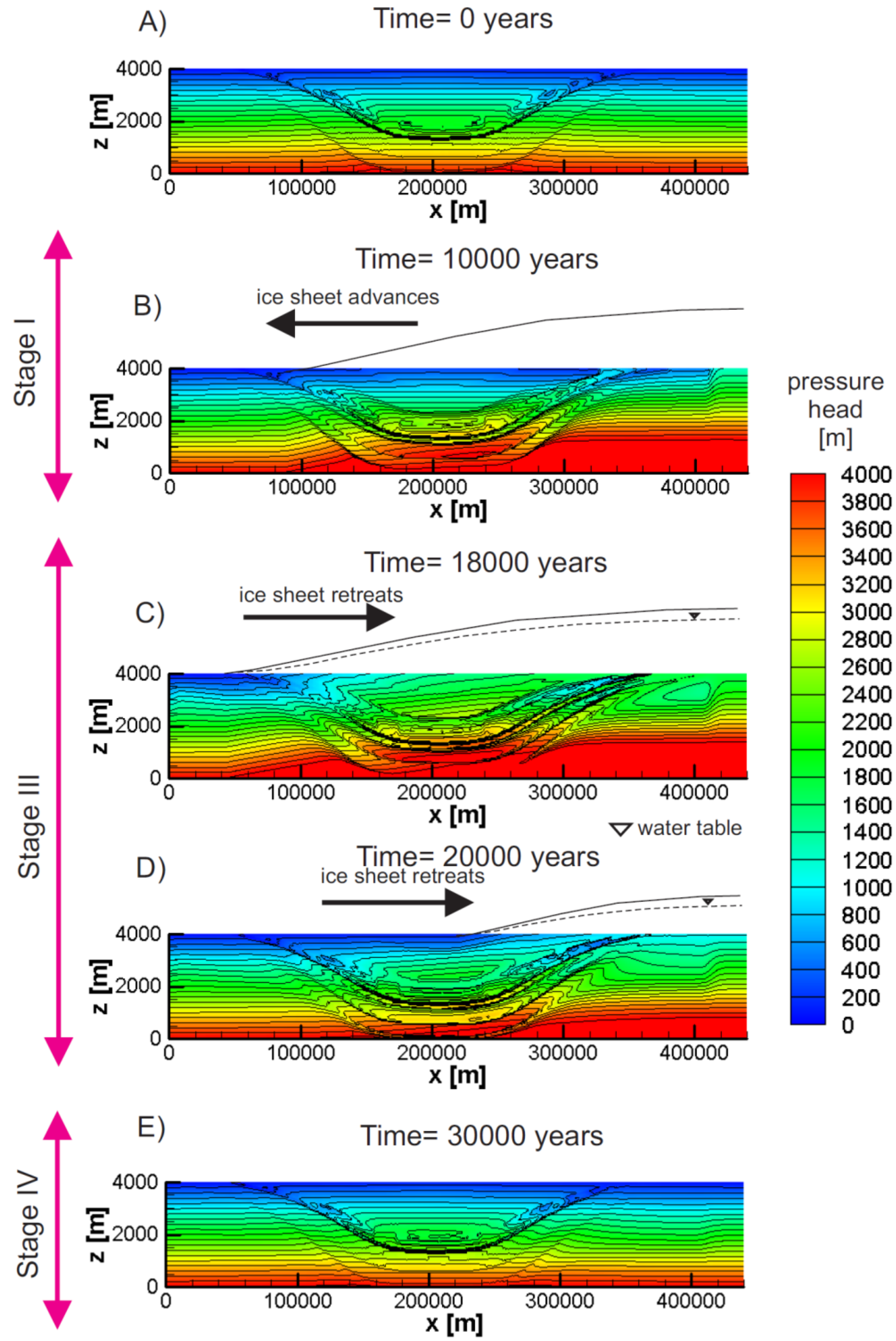

Figure 4. Spatial distribution of point pressure head: A) initial condition, B) 10000 years (Stage I), C) 18000 years (Stage III), D) 20000 years (Stage III), and E) 30000 years (Stage IV)

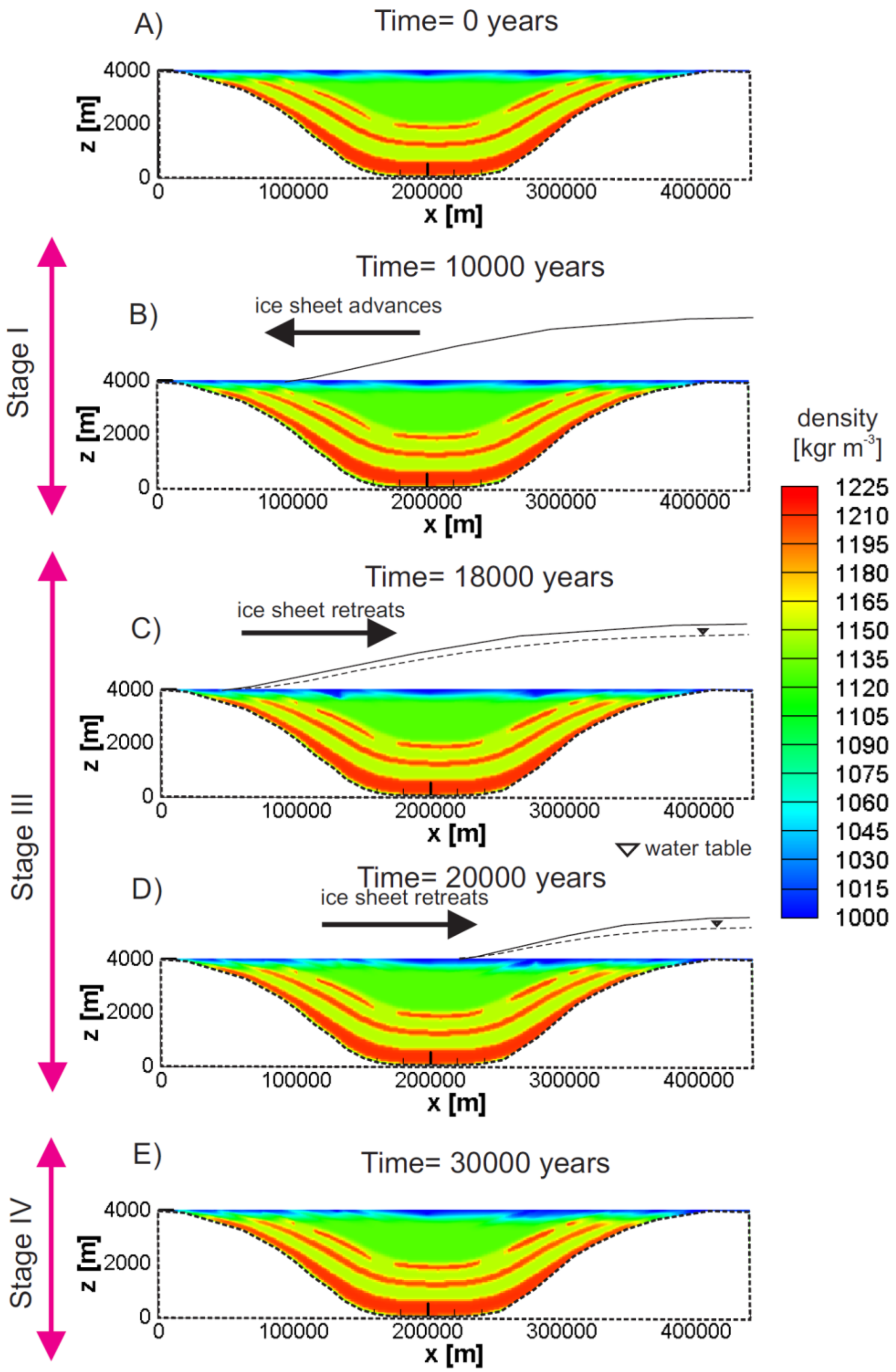

Figure 5. Spatial distribution of fluid density: A) initial condition, B) 10000 years (Stage I), C) 18000 years (Stage III), D) 20000 years (Stage III), and E) 30000 years (Stage IV)

5.2 Geochemical evolution in the hypothetical sedimentary basin

The simulations considered here focus on major ion chemistry involving the components Ca^{2+}, Mg^{2+}, Na^{+}, K^{+}, SO_4^{2-}, Cl^{-}, Br^{-}, CO_3^{2-} and H^{+}, aqueous complexation reactions, ion exchange and mineral dissolution-precipitation. Mineral dissolution and precipitation are expected to be some of the most important geochemical processes in the basin during a glaciation cycle. Mineral reactions may be induced by the displacement of groundwater into a region with a different mineral assemblage than present at its origin, or when waters with different chemical compositions mix. For example, mineral dissolution may be induced by the infiltration of fresh meltwater undersaturated with respect to mineral phases present in the rock matrix (i.e. calcite ($CaCO_3$), dolomite ($CaMg(CO_3)_2$), anhydrite ($CaSO_4$) and halite (NaCl)).

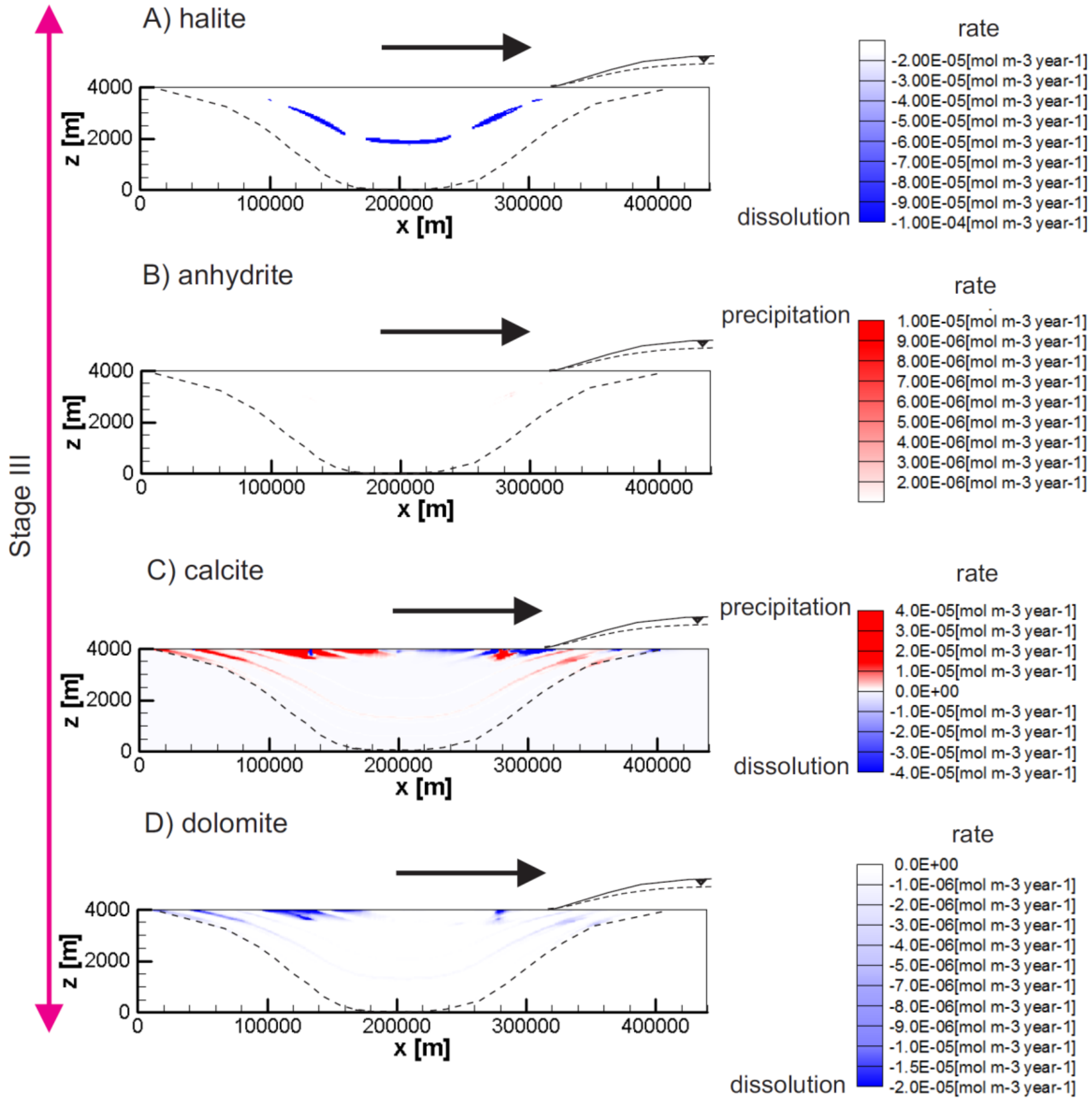

Figure 6. Spatial distribution of mineral reaction rates during Stage III, ice sheet melting (21,000 years): A) halite dissolution, B) anhydrite precipitation, C) calcite precipitation and dissolution, and D) dolomite dissolution

Halite dissolution and calcite precipitation exhibit the largest rates, approximately 10^{-4} mol m^{-3} yr^{-1} and 4 x 10^{-5} mol m^{-3} yr^{-1}, respectively, and are the most spatially extensive mineral reactions in the basin (Figure 6). Halite dissolution is limited spatially to the assumed initial location of this mineral phase (i.e. within the Ev unit, Figures 1 and 3). Diffusive exchange between Dol1, which completely surrounds the Ev unit and in which groundwater is initially undersaturated with respect to halite, is the most probable mechanism driving halite dissolution.

Calcite precipitation rates are greatest in the shallow flanks of the basin (Figure 6C), and are in part related to dedolomitization. Dedolomitization is indicated by the coincident spatial patterns of calcite precipitation and dolomite dissolution which occur, for example, at shallow depths near the basin boundary between units Sand2 and Sh1 (Figure 6C and D). The precipitation rates for calcite are about two times larger than the dissolution rates for dolomite because two moles of calcite are precipitated for each mole of dolomite that is dissolved.

The amount of each mineral dissolved or precipitated during the entire 32500 yr simulation is small relative to the initial volume fractions (i.e. Figure 3). Over the entire simulation the maximum change in mineral volume fractions are: 0.35% for halite dissolution; 0.0013% for anhydrite precipitation; 0.013% and 0.0085% for calcite dissolution and precipitation, respectively; and 0.0072% for dolomite dissolution.

As might be expected, mineral dissolution and precipitation will influence porosity. However, the porosity is influenced not only by mineral reactions, but also by the hydromechanical coupling resulting from loading by the ice sheet. The maximum porosity increase of approximately 0.004 occurs in the Ev unit because of halite dissolution; this unit had an initial porosity that varied with depth from approximately 0.08 to 0.02. The results therefore indicate a porosity enhancement of approximately 5 to 20% in the Ev unit during the course of the simulation. The natural tendency of evaporates to compensate for dissolution-induced porosity changes by deformation and consolidation was not considered in the present simulations. Porosity decreases due to mineral precipitation are negligible (results not shown).

Despite the occurrence of geochemical reactions throughout the basin, the net effect on the solution composition is minimal for the time frames assessed, as evidenced by near constant fluid densities (Figure 5). During ice retreat, a region of low chloride concentration develops to depths of approximately 300 m in the more permeable aquifers (i.e. Sand3, Sand4, and Dol2) which sub-crop beneath the toe of the receding ice sheet (results not shown). Freshening of these shallow aquifers is also indicated by a decrease in dissolved sulfate, calcium and magnesium. However, throughout the majority of the basin the major ion distributions are remarkably stable during the 32500 yr simulation.

6. CONCLUSIONS

The results demonstrate that the newly-developed MIN3P-NWMO code is capable of simulating reactive transport for a two-dimensional cross section of a sedimentary basin (up to 400 km long and 4 km deep) over time periods on the order of 30,000 years. Such simulations can include key geochemical reactions including complexation, ion exchange and mineral dissolution-precipitation, in addition to density-dependent flow, solute transport, and hydromechanical coupling.

In addition to the code evaluation, a hypothetical scenario was developed to investigate the hydrogeological and geochemical stability of a large scale sedimentary basin during a single glaciation-deglaciation cycle. During the period of deglaciation, active groundwater flow in the shallow aquifers increases as a consequence of the infiltration of glacial meltwater below the warm-based glacier. Deeper in the basin, Darcy velocity increases are also noted in the highest hydraulic conductivity units (i.e. sandstones). The results suggest that the low effective hydraulic conductivity and near horizontal layering of the hydrogeological units that form the basin, and the relatively low hydraulic gradients resulting from the geometry of the melting ice sheet, are responsible for no substantial recharge.

From a geochemical perspective, the simulation results reveal that dedolomitization (i.e. dissolution of dolomite ($MgCa(CO_3)_2$) and precipitation of calcite ($CaCO_3$)) is the most significant geochemical process during the deglaciation phase. However, as a consequence of the low flow rates in the sedimentary basin, the net rates of dedolomitization are practically negligible for time scales on the order of 10,000 years and dedolomitization is mainly restricted to the shallow aquifers. Although dissolution of halite (NaCl) is more significant locally (i.e. at the margins of the evaporite units), it is not as widespread as dedolomization. Slight porosity enhancement is predicted as a result of halite dissolution in the evaporite units (Ev); overall, porosity changes due to mineral dissolution-precipitation reactions are predicted to be negligible. In general, the simulation results indicate a high degree of geochemical stability for this hypothetical basin.

Although the spatial discretization of the model allowed for an adequate representation of the sedimentary units, it is likely that the mixing zones of different waters at the interfaces between geological units have not been resolved with sufficient detail. Water-rock interactions in the vicinity of these interfaces will likely occur in a narrower region than captured by the simulations, possibly leading to more pronounced local porosity variations. A parallelized version of MIN3P-NWMO is being developed to provide the computational efficiency required for simulations with finer spatial discretization.

REFERENCES

[1] Grasby, S., K. Osadetz, R. Betcher and F. Render. 2000. Reversal of the regional-scale flow system of the Williston basin in response to Pleistocene glaciation. Geology, 28, 635-638.

[2] Grasby, S. and Z. Chen. 2005. Subglacial recharge into the Western Canada Sedimentary Basin. Impact of Pleistocene glaciation on basin hydrodynamics. GSA Bulletin, 117, 500-514.

[3] McIntosh, J. and L. Walter. 2005. Volumetrically significant recharge of Pleistocene glacial meltwaters into epicratonic basins: Constraints imposed by solute mass balances. Chemical Geology, 222, 292-309.

[4] McIntosh, J. and L. Walter. 2006. Paleowaters in Silurian-Devonian carbonate aquifers: geochemical evolution of groundwater in the great lakes region since the late Pleistocene. Geochimica et Cosmochimica Acta, 70, 2454-2479.

[5] McIntosh, J., G. Garven and J. Hanor. 2011. Impacts of Pleistocene glaciation on large-scale groundwater flow and salinity in the Michigan Basin. Geofluids, 11, 18-13.

[6] Bense, V.F. and M.A. Person. 2008. Transient hydrodynamics within intercratonic sedimentary basins during glacial cycles. Journal of Geophysical Research-Earth Surface, 113, Article No. F04005, 1-17.

[7] Mayer, K.U., E.O. Frind and D.W. Blowes. 2002. Multicomponent reactive transport modeling in variably saturated porous media using a generalized formulation for kinetically controlled reactions, Water Resour. Res., 38, 1174, doi: 10:1029/2001WR000862.

[8] Henderson, T., K.U. Mayer, B. Parker and T. Al. 2009. Three-dimensional density-dependent flow and multicomponent reactive transport modeling of chlorinated solvent oxidation by potassium permanganate. Journal of Contaminant Hydrology, 106, 195-211.

[9] Harvie, C.E., N. Moller and J.H. Weare. 1984. The prediction of mineral solubilities in natural waters: The Na-K-Mg-Ca-H-Cl-SO_4-OH-HCO_3-CO_3-CO_2-H_2O system to high ionic strengths at 25^oC. Geochimica et Cosmochimica Acta, 48, 723-751.

[10] Pitzer, K.S. 1973. Thermodynamics of electrolytes. I. Theoretical basis and general equations. Journal of Physical Chemistry, 77, 268-277.

[11] Monnin, C. 1994. Density calculation and concentration scale conversions for natural waters. Computers & Geosciences, 20, 1435-1445.

[12] Neuzil, C. 2003. Hydromechanical coupling in geologic processes. Hydrogeology Journal, 11, 41-83.

[13] Voss, C. and A. Provost. 2008. SUTRA-A model for saturated-unsaturated, variable-density ground-water flow with solute or energy transport. U.S. Geological Survey Water-Resources Investigations Report 02-4231, 250p.

[14] Bea, S.A., K.U. Mayer and K.T.B. MacQuarrie. 2011. Modelling reactive transport in sedimentary rock environments - Phase II, MIN3P code enhancements and illustrative simulations for a glaciation scenario, NWMO Technical Report, in review.

[15] Normani, S. 2009. Paleoevolution of pore fluids in glaciated geologic settings. PhD dissertation, University of Waterloo, Waterloo, Ontario, Canada.

[16] Medina, C., J. Ruppa and D. Barnes. 2011. Effects of reduction in porosity and permeability with depth on storage capacity and injectivity in deep saline aquifers: A case study from the Mount Simon Sandstone aquifer. International Journal of Greenhouse Gas Control, 5, 146-156.

[17] Sykes, J., E. Sykes, S. Normani, Y. Yin and Y.-J. Park. 2008. Phase I hydrogeologic modelling. University of Waterloo, OPG 00216-REP-01300-00009-R00.

[18] Harrison, W., G. Grammer and D. Barnes. 2009. Reservoir characteristics of the Bass Islands dolomite in Otsego County, Michigan: Results for a saline reservoir CO_2 sequestration demonstration. Environmental Geosciences, 16, 139-151.

[19] Westjohn, D. and T. Weaver. 1998. Hydrogeologic framework of the Michigan Basin regional aquifer system. U.S. Geological Survey Professional Paper PP 1418.

[20] Avis, J., R. Roberts, D. Chace, N. Toll and R. Beauheim. 2009. Hydraulic testing to characterize low permeability sedimentary formations - proposed Deep Geologic Repository, Tiverton, Ontario. Proceedings GeoHalifax 2009, 62nd Canadian Geotechnical Conference & 10th Joint CGS/IAH-CNC Groundwater Conference, 1356-1361.

[21] Raven, K., K. Novakowski, R. Yager and R. Heystee. 1992. Supernormal fluid pressures in sedimentary rocks of southern Ontario-western New York State. Canadian Geotechnical Journal, 29, 80-93.

[22] Birkholzer, J. and Q. Zhou. 2009. Basin-scale hydrogeologic impacts of CO_2 storage: Capacity and regulatory implications. International Journal of Greenhouse Gas Control, 745-756.

[23] Person, M., J. Raffensperger, S. Ge and G. Garven. 1996. Basin-scale hydrogeologic modeling. Reviews of Geophysics, 34, 61-87.

[24] Bahr, D.B., E.W.H. Hutton, J.P.M. Syvitski and L.F. Pratson. 2001. Exponential approximations to compacted sediment porosity profiles. Computers & Geosciences, 27, 691-700.

[25] Person, M., J. McIntosh, V. Bense and V.H. Remenda. 2007. Pleistocene hydrology of North America: The role of ice sheets in reorganizing groundwater flow systems. Reviews of Geophysics, 45, RG3007, 1-28.